SIMULATING SUB-WAVELENGTH TEMPORAL EFFECTS IN A SEEDED FEL DRIVEN BY LASER-ACCELERATED ELECTRONS

S. I. Bajlekov*, S. M. Hooker, Department of Physics, University of Oxford, OX1 3PU, U.K.
R. Bartolini, John Adams Institute, University of Oxford, OX1 3RH, U.K.
and Diamond Light Source Ltd, Oxfordshire, OX11 0QX, U.K.

Abstract

Ultrashort electron bunches from laser-driven plasma accelerators hold promise as drivers for short-wavelength free electron lasers. While FEL simulation techniques have been successful in simulating lasing at present-day facilities, the novel sources investigated here are likely to violate a number of widely-held assumptions. For instance the HHG seed radiation, as well as the radiation generated by the bunch, may not conform to the slowly-varying envelope approximation (SVEA) on which the majority of codes rely. Additionally, the longitudinal macroparticle binning precludes the modeling of the full physics of the system. In order to more completely simulate the sub-wavelength effects which arise, we have developed an unaveraged 1-D time-dependent code without the SVEA. We use this to perform numerical analyses and highlight some of the additional features that these new systems present. We conclude that while coherent spontaneous emission from ultrashort bunches may significantly affect start-up, the sub-wavelength structure of HHG seeds has little effect.

INTRODUCTION

Progress in the field of laser-plasma wakefield acceleration (LPWA) has opened up the possibility of developing synchrotron radiation sources driven by the electron bunches generated by such devices [1]. Quasi-monoenergetic electron bunches have been accelerated up to $1\,\mathrm{GeV}$ [2], and it is conceivable that further developments could lead to the generation of beams with emittance, energy spread and peak current suitable for FEL operation in the XUV range with relatively short undulator trains [3].

FEL studies [4, 5] have shown that a modest projection of the presently achievable beam parameters would be sufficient to drive a SASE FEL in the XUV or soft x-ray wavelength range. Here we investigate the possibility of seeding the FEL in order to improve the temporal characteristics of the SASE radiation. The operation of an FEL driven by LPWA-generated electrons and seeded with an HHG seed is characterized by the ultrashort electron bunch duration (of order 10 fs), and a seed field that comprises a train of attosecond bursts. Under these conditions, the FEL operation at nm wavelengths, may violate some of the common assumptions on which standard FEL codes (GENESIS [6], GINGER [7]) rely. In fact, the use of the slowly-varying

envelope approximation (SVEA) and the averaging of the trajectories over an undulator period appear questionable.

Analyses of the limits of validity of the SVEA [8, 9] conclude that in the majority of conditions achievable in common LINAC-driven FELs, it is not significantly violated. We revisit this analysis in the context of the LPWA-driven FEL and to this end have developed the unaveraged 1-D code Aurora which does not use the SVEA. In this paper we present the code, a description of the underlying equations and algorithms, and benchmarks against Perseo [10]. We present simulation results of several situations pertinent to LWPA-driven HHG-seeded FELs and compare them to those obtained by identical input parameters in Perseo.

AURORA CODE DESCRIPTION

Aurora shares a number of features with the multi-frequency code MUFFIN by Piovella [11], though it was developed independently. It is written in MATLAB, with the most numerically-intensive subroutines included as MEX libraries written in C. This section gives an overview of its operation.

General Framework

The simulations are performed within a time window of length $N_\lambda \lambda_0$, where λ_0 is the resonant fundamental FEL wavelength and N_λ is the number of wavelengths in the window. The window moves at the velocity of light, c, and hence in this frame the electrons slip behind the radiation at a rate of $(1 - \beta_z)c$, where β_z is the electrons' normalized longitudinal velocity. The boundary conditions are periodic, whereby any electrons escaping through the back of the window re-enter through the front. As the window propagates through the undulator (along z), the evolution of the radiation field and the electron positions and energies are computed. The coordinate within the window is the ponderomotive phase, $\theta = k_0(z - ct)$, where $k_0 = 2\pi/\lambda_0$ is the resonant wavenumber.

The radiation is represented by the on-axis electric field, $E_x(z, \theta)$, polarized along the direction of transverse electron motion. It is recorded on a grid of N_{pts} points per wavelength, allowing a bandwidth of $2\lambda_0/N_{\mathrm{pts}} < \lambda < N_\lambda \lambda_0$. For some computational steps the Fourier transform of the normalized magnetic vector potential, $u = \frac{e}{mc}A_x$, is used instead, with $E_x = -\partial A_x/\partial t$.

The electron bunch is represented by a set of N_{part} macroparticles, each weighted to represent w_i electrons.

* s.bajlekov1@physics.ox.ac.uk

The particles are free to move throughout the window, thereby potentially altering the beam temporal profile. Initial shot-noise microbunching is modeled as in Perseo [12].

A constant transverse bunch cross-section Σ_b is assumed (i.e. no undulator or external focusing) that is matched to the radiation size, while diffraction effects are neglected. The effects of emittance and diffraction can be deduced through Xie's 3-D scalings [13], and implemented as a linear scaling on the gain. The undulator is assumed to be linear, with period λ_u and rms strength parameter a_u.

FEL Equations

The propagation cycle is carried out as follows:

Current density The transverse current density, $J_x(z, \theta)$ is calculated from the macroparticle distribution on the same grid as the radiation field, according to

$$J_x(\theta, z) = \frac{e\sqrt{2}a_u}{\Sigma_b} \cos(k_u z) \sum_{i=1}^{N_{part}} \frac{w_i}{\gamma_i} C(\theta - \theta_i), \quad (1)$$

where e is the elementary charge, $k_u = 2\pi/\lambda_u$ is the undulator wavenumber, i runs over the macroparticle indices and γ_i are the Lorentz factors while θ_i are the ponderomotive phases. The distribution C represents the cloud-in-cell weighing applied to the macroparticles in order to project their distribution onto the grid. We subsequently transform to Fourier space, $\tilde{J}_x(z, k) = \mathcal{F}[J_x(z, \theta)] = \int_{-\infty}^{+\infty} J_x(z, \theta) e^{-i\theta} \, d\theta$, where we convolve with a Gaussian in order to reduce high-frequency noise.

Radiation field We transform the wave equation for the magnetic vector potential, $\partial^2 A_x/\partial z^2 - \frac{1}{c^2}\partial^2 A_x/\partial t^2 = -\frac{1}{\epsilon_0 c^2}J_x$, to the frame of reference moving at c through the substitution $t \to t - z/c$, yielding

$$\left(\frac{\partial^2}{\partial z^2} - \frac{2}{c}\frac{\partial^2}{\partial z \partial t}\right) A_x = -\frac{1}{\epsilon_0 c^2} J_x.$$

We neglect the second derivative with respect to z as it corresponds to a backward-propagating wave [11], which would become unphysical in a periodic domain. Carrying out a Fourier transform and rearranging we obtain

$$\frac{\partial}{\partial z}\tilde{A}_x(z, k) = \frac{1}{2ik}\frac{1}{\epsilon_0 c^2}\tilde{J}_x(z, k), \quad (2)$$

on the basis of which we propagate the radiation field.

Macroparticles The macroparticle energies are propagated in a way similar to that used in Perseo

$$\frac{\partial \gamma_i}{\partial z} = -\frac{\sqrt{2}ea_u}{\gamma_i mc^2} \cos(k_u z) E(z, \theta_i), \quad (3)$$

where m is the electron rest mass. Notably, instead of directly using the ponderomotive phase, the field is included explicitly, allowing the full effect of a broadband field with

FEL Theory

a fast-changing amplitude to be modeled. The macroparticle positions are shifted by

$$\frac{\partial \theta_i}{\partial z} = -\frac{k_0}{2\gamma_i^2}\left(1 + a_u^2\left[1 + \cos(2k_u z)\right]\right). \quad (4)$$

The cosine term corresponds to the oscillation of the electron's longitudinal velocity as its direction of motion alternates. Including this explicitly naturally leads to the emission of odd harmonics of the fundamental. As in Perseo, the magnetic field contribution to Eq. (3) and the electric field contribution to Eq. (4) are neglected.

Benchmarking

We verified Aurora's performance in benchmarks against Perseo. The latter was chosen since in the case of a slowly-varying field envelope, small electron energy spread and no coherent spontaneous emission, the output from Aurora should match Perseo's. Here we present results from a steady-state and a time-dependent SASE benchmark. The nominal electron bunch characteristics, corresponding to projected LPWA values, are given in Table 1 together with the undulator and FEL parameters:

Table 1: Simulation Parameters

Electrons		
Energy	E	320 MeV
	γ	625
Energy spread	σ_E/E	0.1 %
Peak current	I_{pk}	10 kA
Transverse bunch size	σ_x	100 μm
Undulator		
Period	λ_u	0.020 m
rms strength	a_u	0.5
Resonant wavelength	λ	32 nm
Pierce parameter	ρ	0.0041
Gain length	L_G	0.23 m

We found a configuration of $N_{pts} = 256$ and 800 macroparticles per wavelength to be sufficient for good agreement with analytical predictions for the gain length, as well as energy conservation (both within $\sim 0.5\%$). Figure 1 shows a comparison of the results of a steady state simulation, i.e. $N_\lambda = 1$.

A time-dependent SASE benchmark was also performed in a window of $N_\lambda = 500$: the output profiles near saturation are shown in Fig. 2. The phases of the initial shot noise bunching were random, but identical for both codes. The beam current was constant throughout the window. In order to compare the profile of the power output from Aurora to that from Perseo, the E-field was split into slices of length λ_0, and the power carried by the fundamental Fourier component of each slice was evaluated, thus reducing the effective bandwidth to match Perseo's. This reduction was
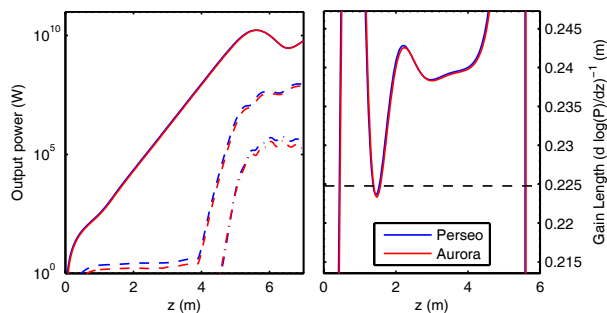
Figure 1: Steady state benchmark of output power and gain length. Solid lines represent emission in the fundamental, dashed lines are 3rd harmonic and dash-dotted are 5th. The horizontal black line is the 1-D analytical gain length for no energy spread.

applied wherever Aurora's electric field needed to be converted to Perseo's wavelength-averaged potential, e.g. for seeding radiation. The plots clearly show that the Aurora output matches that of Perseo in these benchmark cases.
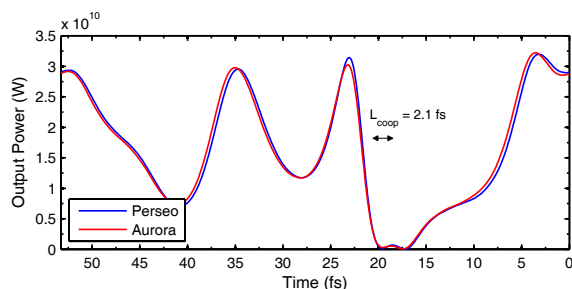

Figure 2: SASE output profiles near saturation ($z = 6.9$ m) at the fundamental. The cooperation length, $L_{\text{coop}} = \lambda_0/4\pi\rho$, is also indicated.

RESULTS

Coherent Spontaneous Emission

Where the electron bunch current profile varies significantly on the scale of the FEL wavelength, coherent spontaneous emission (CSE) occurs in addition to shot noise. As discussed previously, this emission may affect the initial stages of FEL gain [11, 14]. We model this effect for ultra-short bunches, as expected from LPWA, by assuming a Gaussian bunch profile of rms length 10 fs and peak current 10 kA. For these bunches, with other parameters as in Table 1, we see the initial level of micro-bunching increase from shot noise levels of 10^{-5} up to $\sim 10^{-3}$ when Aurora is used to correctly model the current gradient. Figure 3 shows a comparison of simulation results from Perseo and Aurora.

Evidently CSE enables a faster transition from incoherent emission to the exponential gain regime. This is demonstrated most clearly in regions of the bunch where both the
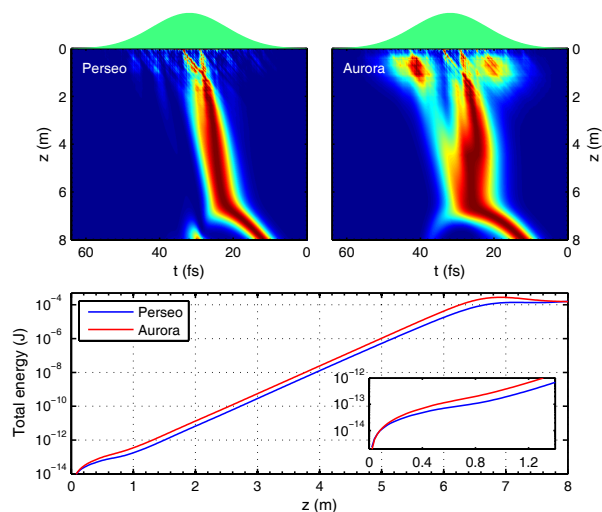

Figure 3: The same bunch profile (green) is used to simulate SASE gain in Perseo and Aurora, shown as output profile (normalized to P_{max} at every z) vs undulator position, in the reference frame of the electron bunch. The additional CSE in Aurora is evident. The bottom plot shows the evolution of total energy within the window vs z, with magnified initial gain.

gradient of current vs time as well as the current itself are high, for instance at the locations of the two spikes in the output profile at $z \approx 0.8$ m. Such effects may be crucial in initial proof-of-principle FEL experiments driven by laser-plasma accelerators, since these FELs are likely to be operating in challenging regions of parameter space where lasing is not straightforward. In this case CSE may be able to "kick-start" the process and lead to detectable gain from a short undulator train. On the other hand, this effect is attenuated as the energy spread increases.

Seeding With High-Harmonics

FEL radiation amplified from noise is not temporally coherent beyond the cooperation length, L_{coop}. It is possible to surpass this by seeding the FEL with high-harmonics of a laser beam, thereby transferring the longitudinal coherence of the laser to the harmonics and subsequently the FEL output. This is of particular interest in the XUV and soft x-ray regime, where suitable seeding is available from high-harmonic generation (HHG) of visible laser radiation. In a gas the harmonics are emitted as a train of attosecond bursts, one for each half-cycle of the driving laser pulse. Since the length of the spikes is often shorter than the resonant FEL wavelength, single-frequency FEL codes may not be able to fully model this seeding process. We therefore carried out a comparison of the effect of a train of attosecond pulses as simulated by Perseo and by Aurora.

Without special measures to preserve the attosecond structure, it is washed out into a longer pulse of length $\geq L_{\text{coop}}$ during FEL gain [15]. We are therefore interested in whether the details of the structure make a differ-

ence prior to this stage. We carried out a series of simulations using idealized pairs of bursts at 32 nm, i.e. the 25th harmonic of a single cycle of an 800 nm CW driving laser: on a periodic grid this corresponds to an electron beam being seeded by a continuous train of bursts. These had Lorentzian temporal profiles of length 50, 100 and 200 attoseconds FWHM. The field amplitude was scaled so that the mean power within the reduced fundamental bandwidth was $P_{\text{seed}} = 37.5$ kW. Hereby shorter spikes carried more total energy due to their greater total bandwidth, but less energy within the gain bandwidth $\Delta\lambda/\lambda = \rho$. Accordingly, as seen in Fig. 4, simulations seeded by shorter spikes entered the exponential gain regime further into the undulator. More notable is the fact that the results obtained by Perseo are practically identical to those obtained by Aurora, despite the slowly-varying envelope approximation and electron motion averaging employed by the former.
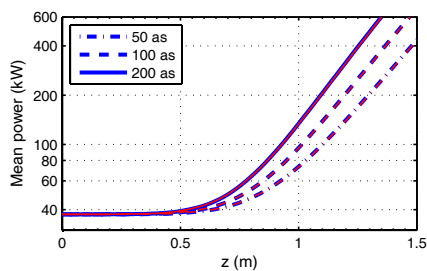

Figure 4: Amplification of HHG seeds with different burst durations. Perseo results are plotted in blue (thicker lines) and Aurora in red. Electron beam characteristics are given in Table 1.

Furthermore, we obtained a numerical solution to Lewenstein's equations for high-harmonic generation [16] from an 800 nm laser pulse of intensity 5×10^{14} W cm^{-2} and FWHM duration 50 fs. Harmonic orders 1 through 11 were filtered out and the HHG seed was scaled so as to have 12.6 nJ is in the 25th harmonic at 32 nm (and total energy 630 nJ). We used this as the seed field in Perseo and Aurora simulations, with the results shown in Fig. 5. We observe negligible difference between the output profiles from both. It appears possible to accurately simulate seeding using broadband radiation pulses using single-frequency codes such as Perseo. We attribute this to the strong mode selection that takes place during FEL gain.

CONCLUSION

We have described the unaveraged time-dependent 1-D code Aurora, working outside the slowly-varying envelope approximation. We presented benchmarks of the code against Perseo, which is equivalent to Aurora in the limit of a slowly varying radiation envelope and no beam current variations on the scale of a radiation wavelength. In further simulations we showed that coherent spontaneous emission due to the micron-scale length predicted for laser-accelerated driving electron bunches may significantly en-
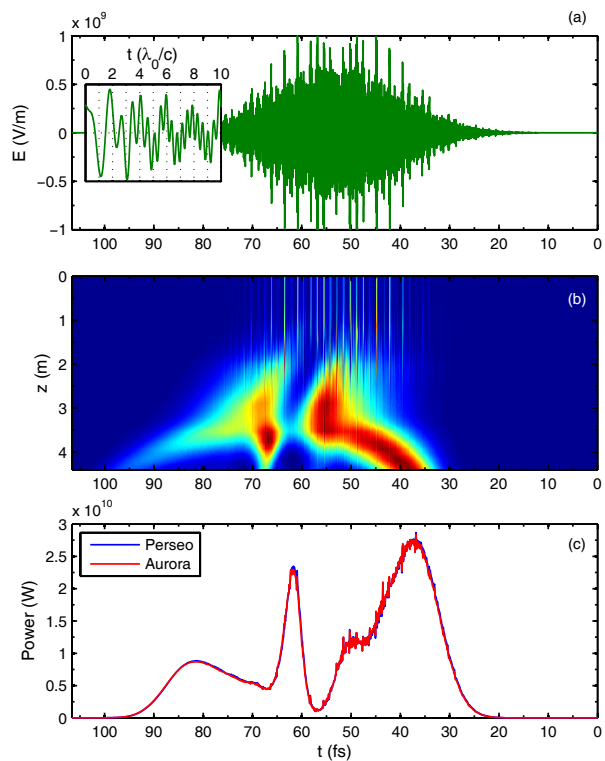

Figure 5: (a) Electric field profile of seed, with sub wavelength variations at $t \approx 60$ as (inset). (b) Evolution of normalized output profile for Aurora, shown in the reference frame of the radiation (i.e. the electrons are slipping to the left), and (c) profiles of power in the fundamental near saturation at $z = 4$ m.

hance the start-up process. On the other hand, we found the SVEA to be sufficient to describe the FEL dynamics in the regime where an HHG seed with sub-wavelength structure is used.

REFERENCES

[1] H. P. Schlenvoigt *et al.*, *Nature Phys.* **4**, 130 (2007).

[2] W. P. Leemans *et al.*, *Nature Phys.* **2**, 696 (2006).

[3] F. Grüner *et al.*, *Appl. Phys. B* **86**, 431 (2007).

[4] V. Petrillo *et al.*, *Phys. Rev. STAB* **11**, 070703 (2008).

[5] S. I. Bajlekov *et al.*, *FEL'08*, MOPPH081 (2008).

[6] S. Reiche, *Nucl. Inst. Meth. A* **429**, 243 (1999).

[7] W. M. Fawley, *LCLS-TN-04-03* (2004).

[8] R. Bonifacio *et al.*, *Opt. Commun.* **101**, 185 (1993).

[9] W. M. Fawley, *PAC'09*, TU1PBI04 (2009).

[10] L. Giannessi, *FEL'06*, MOPPH026 (2006).

[11] N. Piovella, *Phys. Plasmas* **6**, 3358 (1999).

[12] L. Giannessi, *FEL'04*, MOPOS26 (2004).

[13] M. Xie, *Nucl. Inst. Meth. A* **445**, 59 (2000).

[14] B. W. McNeil *et al.*, *Opt. Commun.* **165**, 65 (1999).

[15] L. Giannessi, *FEL'06*, MOCAU05 (2006).

[16] M. Lewenstein *et al.*, *Phys. Rev. A* **49**, 2117 (1994).